Title	Magnetic and nematic orderings in spin-1 antiferromagnets with single-ion anisotropy
Author(s)	Wierschem, Keola; Kato, Yasuyuki; Nishida, Yusuke; Batista, Cristian D.; Sengupta, Pinaki
Citation	Weickert, F., Küchler, R., Steppke, A., Pedrero, L., Nicklas, M., Brando, M., et al. (2012). Low-temperature thermodynamic properties near the field-induced quantum critical point in NiCl2-4SC(NH2)2. Physical Review B, 85(18), 184408-.
Date	2012
URL	http://hdl.handle.net/10220/10213
Rights	© 2012 American Physical Society. This paper was published in Physical Review B and is made available as an electronic reprint (preprint) with permission of American Physical Society. The paper can be found at the following official DOI: [http://dx.doi.org/10.1103/PhysRevB.86.201108]. One print or electronic copy may be made for personal use only. Systematic or multiple reproduction, distribution to multiple locations via electronic or other means, duplication of any material in this paper for a fee or for commercial purposes, or modification of the content of the paper is prohibited and is subject to penalties under law.

PHYSICAL REVIEW B **86**, 201108(R) (2012)

Magnetic and nematic orderings in spin-1 antiferromagnets with single-ion anisotropy

Keola Wierschem,[1] Yasuyuki Kato,[2] Yusuke Nishida,[2] Cristian D. Batista,[2] and Pinaki Sengupta[1]
[1]*School of Physical and Mathematical Sciences, Nanyang Technological University, 21 Nanyang Link, Singapore 637371*
[2]*T-Division and CNLS, Los Alamos National Laboratory, Los Alamos, New Mexico 87545, USA*
(Received 4 September 2012; published 30 November 2012)

We study a spin-1 Heisenberg model with exchange interaction J, uniaxial single-ion exchange anisotropy D, and Zeeman coupling to a magnetic field B parallel to the symmetry axis. We compute the $(D/J, B/J)$ quantum phase diagram for square and simple cubic lattices by combining analytical and quantum Monte Carlo approaches, and find a transition between XY antiferromagnetic and ferronematic phases that spontaneously break the $U(1)$ symmetry of the model. In the language of bosonic gases, this is a transition between a Bose-Einstein condensate (BEC) of single bosons and a BEC of pairs. Our work opens up new avenues for measuring this transition in real magnets.

DOI: 10.1103/PhysRevB.86.201108 PACS number(s): 75.30.Kz, 02.70.Ss, 75.30.Gw

The unambiguous realization of BECs in laser cooled collections of cold atoms[1,2] triggered the search for more exotic states of matter and phase transitions that take place in bosonic gases. In parallel with these efforts, other experimental groups demonstrated that several aspects of the BEC quantum phase transition can also be measured in quantum magnets that are alternative realizations of bosonic gases.[3–7] The main advantage of this alternative approach is that the much lighter boson mass leads to much higher transition temperatures, while the uniform character and well-defined temperature of quantum magnets are crucial for the study of quantum phase transitions. The main disadvantage is that the continuous symmetry associated with particle number conservation in atomic gases is always an idealization for the case of quantum magnets.[8] However, many real magnets, for which the continuous symmetry breaking terms are much smaller than the ordering temperature, allow for measuring the universal behavior of *continuous symmetry* breaking critical points over a large window of temperatures. The simplest example is the magnetic field induced BEC quantum critical point (QCP) that is observed in several quantum magnets.[3–7]

$S = 1$ magnets can be mapped into gases of semihard-core bosons via a generalization of the Matsubara-Matsuda transformation[9,10] that also maps the local magnetization into the boson density $n_j = S_j^z + 1$. In contrast to the hard-core bosons associated with $S = 1/2$ magnets, it is possible to study "Hubbard-like" bosonic gases with on-site density-density interactions because $n_j \leqslant 2$.[11–15] Moreover, the semihard-core constraint $n_j \leqslant 2$ can be incorporated as an infinitely repulsive three-body on-site term that precludes phase segregation when the two-body term is attractive. This situation is ideal for studying transitions between single-boson BECs and BECs of pairs, whose counterparts in atomic physics are transitions between BECs of atoms and diatomic molecules (transitions between XY magnetic and nematic orderings in the spin language).

While the XY terms of the exchange interaction play the role of the kinetic energy, the Ising terms map into off-site density-density interactions. On-site density-density interactions are generated by uniaxial single-ion anisotropy terms of the form $D(S_j^z)^2$. A magnetic field B, parallel to the symmetry axis, acts as a chemical potential because it couples to the total magnetization $M_z = \sum_j S_j^z$ that coincides with the total number of bosons up to an irrelevant constant. Previous works have exploited this spin-boson mapping for studying spin supersolid phases of $S = 1$ Heisenberg models with uniaxial exchange and single-ion anisotropies.[16–18] The main purpose of this work is to study the quantum phase diagram (QPD) of the isotropic $S = 1$ Heisenberg model when the single-ion anisotropy and Zeeman terms are included. This model is relevant for describing several Ni-based organic compounds as well as inorganic systems that are discussed at the end of this work.

Our $S = 1$ model is defined on a hypercubic lattice,

$$\mathcal{H} = J \sum_{\langle i,j \rangle} \boldsymbol{S}_i \cdot \boldsymbol{S}_j + D \sum_i \left(S_i^z\right)^2 - B \sum_i S_i^z, \qquad (1)$$

and the antiferromagnetic (AFM) exchange coupling $J > 0$ only connects nearest-neighbor sites $\langle i, j \rangle$. Since an attractive on-site interaction is needed for pairing the bosons, we will only consider the $D < 0$ case that corresponds to easy-axis anisotropy.

Hamer *et al.* computed the mean field QPD of $\mathcal{H}$ on a square lattice and obtained a single phase transition from AFM Néel (AFM-z) to the fully polarized (FP) state for large $|D|/J$ values.[19] However, an intermediate nematic phase must exist in this regime according to the effective low-energy model $\tilde{\mathcal{H}}$ that is derived by expanding in the small parameter $J/|D|$ (strong coupling expansion in the bosonic language). The low-energy subspace $\mathcal{S}$ is a direct product of the $S^z = \pm 1$ doublets of each lattice site that are separated from the $S^z = 0$ states by an energy gap $|D|$.[20] $\tilde{\mathcal{H}}$ is obtained by applying a canonical transformation and projecting into $\mathcal{S}$: $\tilde{\mathcal{H}} = P_{\mathcal{S}} e^{\kappa} \mathcal{H} e^{-\kappa} P_{\mathcal{S}}$ (κ is the anti-Hermitian generator of the canonical transformation and $P_{\mathcal{S}}$ is the projector on $\mathcal{S}$). If we use a pseudospin $s = 1/2$ variable to describe each doublet $S^z = 2s^z$, we obtain the following expression for $\tilde{\mathcal{H}}$ up to quadratic order in J:

$$\tilde{\mathcal{H}} = \sum_{\langle ij \rangle} \mathcal{J}^z s_i^z s_j^z + \mathcal{J}^{xy}\left(s_i^x s_j^x + s_i^y s_j^y\right) - 2B \sum_j s_j^z, \qquad (2)$$

with $\mathcal{J}^z = 4J - J^2/D$ and $\mathcal{J}^{xy} = J^2/D$. $\tilde{\mathcal{H}}$ is an $s = 1/2$ XXZ model whose QPD is well known in any dimension. In particular, the mean field phase diagram is qualitatively and quantitatively correct for spatial dimension $d \geqslant 2$. Since the case of interest corresponds to effective

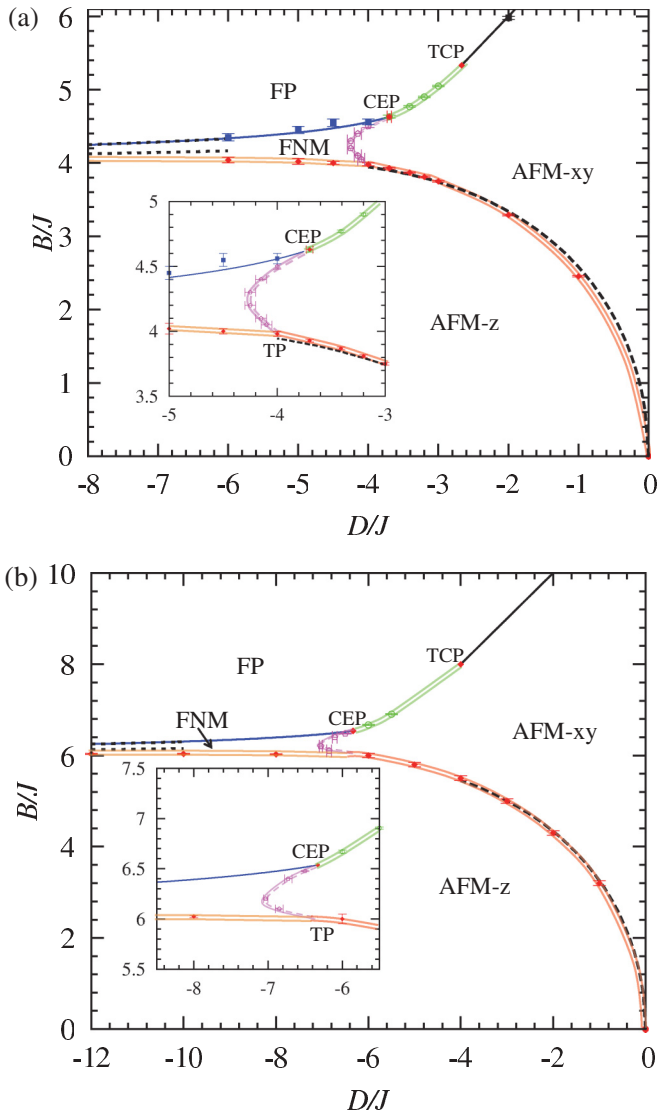

FIG. 1. (Color online) Quantum phase diagrams in (a) square lattice and (b) cubic lattice. Double and single solid lines correspond to first and second order phase transitions, respectively. Single solid lines are obtained by exact solutions, while double solid lines are guides for the eye based on QMC results. Insets: Enlarged views of the FNM to AFM-xy transition. Dashed and dotted lines are analytical solutions for the weak and strong anisotropy regimes, respectively.

strong easy-axis anisotropy $|\mathcal{J}^z/\mathcal{J}^{xy}| \simeq 4|D|/J \gg 1$, the low field ground state has Néel ordering that extends up to the spin-flop field $B_{\rm sf}$ whose mean field value is $B_{\rm sf} \simeq d\sqrt{(\mathcal{J}^z+\mathcal{J}^{xy})(\mathcal{J}^z-\mathcal{J}^{xy})}/2$. The corresponding curve is the lower dotted line on the left of Figs. 1(a) and 1(b). At $B = B_{\rm sf}$, the pseudospin variables flop from the Néel state to a canted ferromagnetic state ($\mathcal{J}^{xy} < 0$) whose canting angle relative to the z axis is given by $\cos\alpha_{\rm sf} = 2\langle s_j^z\rangle = \sqrt{(\mathcal{J}^z+\mathcal{J}^{xy})/(\mathcal{J}^z-\mathcal{J}^{xy})}$. The effective operator for S_j^{+2} is $\widetilde{S_j^{+2}} = P_{\mathcal{S}} e^{\kappa} S_j^{+2} e^{-\kappa} P_{\mathcal{S}} = 2s_j^+$. This identity implies that the planar ferromagnetic ordering in the pseudospin variables or "spin-flop" phase corresponds to ferronematic (FNM) ordering in the original $S = 1$ spin variables, that is, $\langle s_j^+\rangle \neq 0$ implies $\langle S_j^{+2}\rangle \neq 0$. On the other hand, the effective operator for S_j^+ is equal to zero ($\widetilde{S_j^+} = P_{\mathcal{S}} e^{\kappa} S_j^+ e^{-\kappa} P_{\mathcal{S}} = 0$) because of the following symmetry argument. Being odd under time reversal symmetry, $\widetilde{S_j^+}$ must be equal to a polynomial form that only contains odd terms in the s_l^ν variables $\nu = \{x,y,z\}$. Such polynomial form must be odd under a π spin rotation along the z axis because $e^{i\pi\sum_l S_l^z} S_j^+ e^{-i\pi\sum_l S_l^z} = -S_j^+$. Since $e^{i\pi\sum_l S_l^z} s_j^+ e^{-i\pi\sum_l S_l^z} = s_j^+$, the polynomial form must be equal to zero, implying absence of planar magnetic ordering in the large D/J limit and confirming the FNM character of the intermediate phase. The transition to the fully saturated state is of second order in this regime and belongs to the BEC universality class in dimension $d+2$. A mean field treatment[19] of the original Hamiltonian $\mathcal{H}$ misses the second order fluctuations in J ($\mathcal{J}^{xy} = J^2/D$) that stabilize the FNM phase.

The approximated value of the saturation field is

$$B_{\rm sat}(|D|/J \gg 1) \simeq \frac{d}{2}(\mathcal{J}^z - \mathcal{J}^{xy}) = d\left(2J - \frac{J^2}{D}\right), \qquad (3)$$

and the corresponding curve is the upper dotted line on the left of Figs. 1(a) and 1(b). While Eq. (3) is a good approximation for $B_{\rm sat}$ if $|D|/J \gg 1$, the exact curve $B_{\rm sat}(|D|/J \gg 1)$ can be computed analytically as long as the transition remains continuous. By solving the two-body problem of diagonalizing $\mathcal{H}$ in the $M^z = N-2$ invariant subspace (two flipped spins relative to the FP state), we obtain the exact energy $E_g(M^z = N-2)$ of the two bosons bound state. The condensation of these pairs leads to the FNM ordered state. If the transition is continuous, the exact value of $B_{\rm sat}$ is the field such that $E_g(M^z = N-2) = E_g(M^z = N) = N(Jd + D - B)$. The resulting curve is shown as a full line in the $|D|/J \gg 1$ region of Figs. 1(a) and 1(b).

The opposite limit $|D|/J \ll 1$ is well described by a mean field treatment of the original Hamiltonian $\mathcal{H}$. The mean field Néel state $|\Psi_{\rm N}\rangle = \bigotimes_{j\in A}|1\rangle_j \bigotimes_{l\in B}|\bar{1}\rangle_l$ is the most stable at low-enough fields. Here A and B denote the two sublattices, while $|1\rangle_j$, $|\bar{1}\rangle_j$, and $|0\rangle_j$ are the eigenvectors of S_j^z with eigenvalues 1, -1, and 0, respectively. In this regime there is a spin-flop transition, but to a canted XY AFM (AFM-xy) phase that is described by the mean field state

$$|\Psi_{\rm sf}\rangle = \bigotimes_j e^{i\boldsymbol{Q}\cdot\boldsymbol{r}_j}\sin\theta[\cos\phi|1\rangle_j + \sin\phi|\bar{1}\rangle_j] + \cos\theta|0\rangle_j,$$

where $\boldsymbol{Q}$ is the AFM wave vector that has all the components equal to π. The optimal variational parameters θ_0 and ϕ_0 are obtained by minimizing the mean field energy $\langle\Psi_{\rm sf}|\mathcal{H}|\Psi_{\rm sf}\rangle$. The dashed line on the right of Figs. 1(a) and 1(b) corresponds to the spin flop curve $B_{\rm sf}(D/J)$ that results from $\langle\Psi_{\rm N}|\mathcal{H}|\Psi_{\rm N}\rangle = \langle\Psi_{\rm sf}(\theta_0,\phi_0)|\mathcal{H}|\Psi_{\rm sf}(\theta_0,\phi_0)\rangle$.

For small D/J, the second order transition between the spin-flop and FP states belongs to the BEC universality class. The exact value of the saturation field in this regime is shown as a full line in the upper right region of Figs. 1(a) and 1(b), and given by the equation

$$B_0 = D + 4dJ. \qquad (4)$$

However, we know that the effective interaction between bosons should become attractive for $|D| > |D_{c1}|$. Therefore,

the second order transition line described by Eq. (4) should become of first order at a tricritical point (TCP) with coordinates $[D_{c1}/J, B_0(D_{c1}/J)/J]$ [see Figs. 1(a) and 1(b)]. The region near the TCP is well described by the Ginzburg-Landau (GL) free-energy density

$$f(\phi) = (B - B_0)|\phi|^2 + u|\phi|^4 + w|\phi|^6. \tag{5}$$

Here ϕ is the complex order parameter for the BEC of single bosons. u and w are the amplitudes of the effective two-body and three-body interactions in the long wavelength (or continuum) limit. The field induced transition is continuous for repulsive $u > 0$ and it happens at $B_{\rm sat} = B_0$ [see Eq. (4)]. However, it is clear from Eq. (5) that the transition becomes discontinuous for $u < 0$. In this case, the transition field is $B_{\rm sat} = B_0 + u^2/4w$ and the discontinuous change of the boson density is $\Delta m_z = \Delta|\phi|^2 = -u/2w$ ($m_z = \sum_j \langle S_j^z\rangle/N$). The amplitude u changes sign when the two-boson scattering length a_s diverges in $d = 2$ ($a_s \to \infty$) and becomes equal to zero in $d = 3$ ($a_s = 0$). These conditions determine the values of D_{c1}/J in $d = 2$ and $d = 3$, respectively, that can be obtained by computing the effective interaction vertex in the long wavelength and low frequency limits:

$$\Gamma_{\boldsymbol{q}}(\boldsymbol{k},\boldsymbol{k}';\omega) = V_{\boldsymbol{q}}(\boldsymbol{k}) + \int_{-\pi}^{\pi} \frac{d^d p}{(2\pi)^d} \frac{V_{\boldsymbol{q}-\boldsymbol{p}}(\boldsymbol{k})\Gamma_{\boldsymbol{p}}(\boldsymbol{k},\boldsymbol{k}';\omega)}{\omega - \epsilon_{\boldsymbol{k}+\boldsymbol{p}} - \epsilon_{\boldsymbol{k}'-\boldsymbol{p}} + i\delta}, \tag{6}$$

where $V_{\boldsymbol{q}}(\boldsymbol{k}) = 2D + \gamma_{\boldsymbol{q}} + (\sqrt{2} - 2)(\gamma_{\boldsymbol{k}+\boldsymbol{q}} + \gamma_{\boldsymbol{k}})$, $\epsilon_{\boldsymbol{q}} = (2dJ + \gamma_{\boldsymbol{q}})$ is the single boson dispersion at the TCP and $\gamma_{\boldsymbol{q}} = 2J\sum_\nu \cos k_\nu$. By solving Eq. (6) for $\boldsymbol{q} = 0$, $\boldsymbol{k} = \boldsymbol{k}' = \boldsymbol{Q}$, and $\omega \to 0$, we obtain $|D_{c1}|/J = 4d/3$. A similar analysis cannot be applied to the point where the FP phase boundary changes from second to first order coming from the strongly anisotropic side $|D| \gg J$. Note that the FNM phase disappears right at this critical $D = D_{c2}/J$ point (see Fig. 1), while the magnetization vs field curve becomes discontinuous (see insets of Figs. 2 and 3). This discontinuity indicates that it is a critical end point (CEP) and the effective

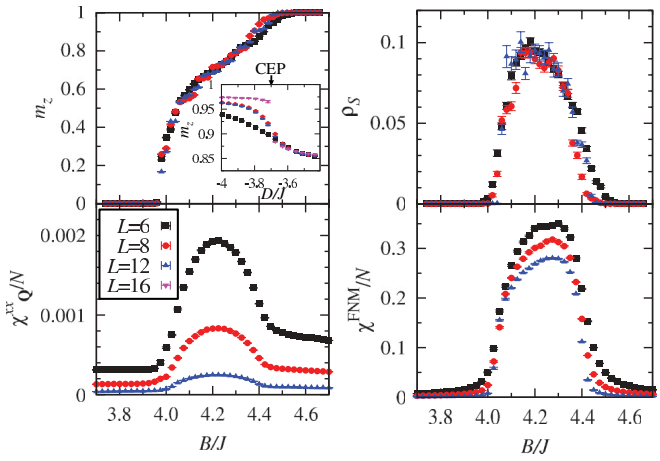

FIG. 2. (Color online) Magnetic field sweep showing AFM-z to FNM to FP sequence of ground states for $d = 2$ lattices of L^2 sites and periodic boundary conditions (PBC). Data shown are for $D/J = -5$ and inverse temperature of $\beta J = 4L$. The inset shows m_z along the line $B(D/J)$ where the two-magnon ground state is degenerate with the FP state.

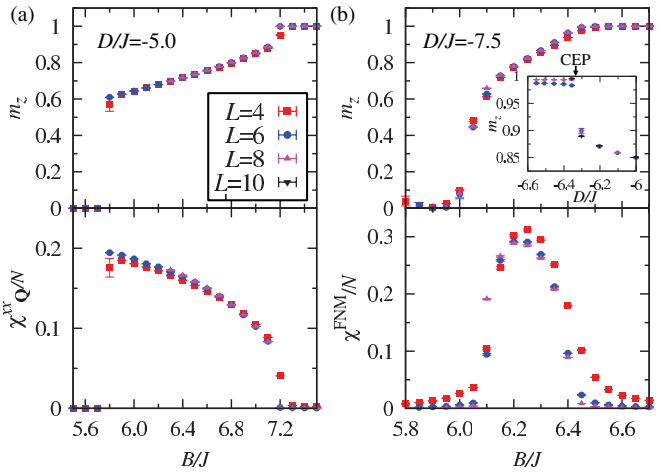

FIG. 3. (Color online) QMC results for $d = 3$ lattices of L^3 spins with PBC. The temperature is scaled with the systems size $\beta J = 4L$ and the Hamiltonian parameters are (a) $D/J = -5$ and (b) $D/J = -7.5$. Inset of (b) shows m_z along the line $B(D/J)$ where the two-magnon ground state is degenerate with the FP state ($\beta J = 6L$).

GL theory is not applicable. Then, the coordinates of the CEP must be obtained from the quantum Monte Carlo (QMC) simulations that we describe below.

Our analysis of the two opposite regimes $|D|/J \gg 1$ and $|D|/J \lesssim 1$ indicates that there is a transition between AFM-xy and FNM orderings in the intermediate region. We use a QMC method with global updates[21] for studying this regime, because there is no small parameter for validating an analytical approach. Although $\mathcal{H}$ does not have a negative sign problem, standard QMC algorithms cannot output the off-diagonal FNM correlator because of a slowing down problem. Therefore, we use a novel multidiscontinuity algorithm[22] that is based on the directed-loop algorithm[23] and eliminates the problem.

The different phases are characterized by computing the zero frequency AFM-xy and FNM susceptibilities,

$$\chi^{xx}_{\boldsymbol{Q}} = \frac{1}{\beta N}\sum_{i,j}\int_0^\beta \langle S_i^+(\tau)S_j^-(0)\rangle e^{i\boldsymbol{Q}\cdot(\boldsymbol{r}_i - \boldsymbol{r}_j)}d\tau,$$

$$\chi^{\rm FNM} = \frac{1}{\beta N}\sum_{i,j}\int_0^\beta \langle S_i^+(\tau)S_i^+(\tau)S_j^-(0)S_j^-(0)\rangle d\tau,$$

where $N = L^d$ is the number of lattice sites. We also compute standard thermodynamic quantities, like the magnetization m_z and the spin stiffness ρ_s (response of the system to a twist in the boundary conditions), that is obtained from the fluctuations of the world lines winding numbers along the principal axes.[24]

Figures 1(a) and 1(b) include the $d = 2$ and $d = 3$ QPDs obtained from our QMC results. Figure 2 shows the four different observables computed as a function of B/J for $D/J = -5$ and different system sizes. Except for the FNM-AFM-xy transition, the phase boundaries of the first order phase transitions [shown in Figs. 1(a) and 1(b)] are determined from the size dependence of the discontinuity of the uniform magnetization and the corresponding kink in the energy density. These boundaries agree very well with

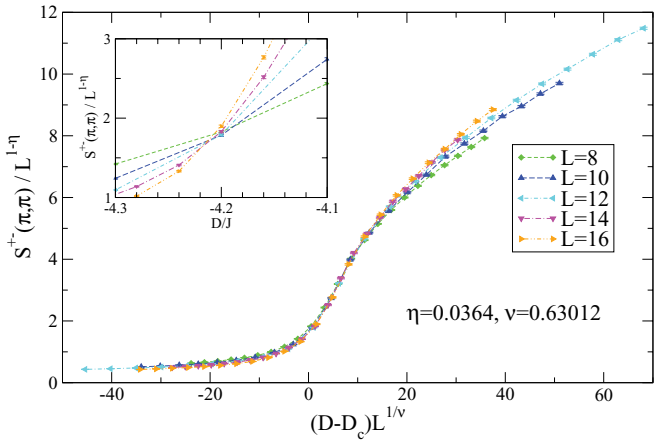

FIG. 4. (Color online) Finite size scaling of the QMC results for the AFM-xy structure factor $S^{+-}(\boldsymbol{Q}) = \sum_{jl} S_j^+ S_l^- e^{i\boldsymbol{Q}\cdot(\boldsymbol{r}_j - \boldsymbol{r}_l)}/N$ near the FNM to AFM-xy transition in $d = 2$ with $B/J = 4.1$ and $\beta = 4L$. The values of the exponents for the Ising universality class in dimension $3 = 2 + 1$ are extracted from Ref. [25]. The common crossing point at $D_c/J = -4.22 \pm 0.02$ (see inset), together with the curve collapse in the critical region, suggests that the transition is continuous.

our analytical solutions in the limiting regimes $|D|/J \gg 1$ and $|D|/J \lesssim 1$. Moreover, the QMC results indicate that the transition to the saturated state becomes of first order between the CEP and TCP that we discussed above. The coordinates of the TCP coincide with the exact values obtained by solving Eq. (6). The coordinates of the CEP obtained from our QMC simulations are $D_{c2}/J = -3.70 \pm 0.03$ for $d = 2$ and $D_{c2}/J = -6.33 \pm 0.03$ for $d = 3$. Figures 3(a) and 3(b) show that the magnetization curve has a small discontinuity for $D/J = -5$, while it is continuous for $D/J = -7.5$. The first order transition line for $|D_{c1}| < |D| < |D_{c2}|$ falls consistently above the curves given by Eqs. (3) and (4), as expected from our GL analysis near the TCP.

The transition from FNM to AFM-xy ordering [double full-dashed line in Figs. 1(a) and 1(b)] spontaneously breaks the discrete symmetry of global spin rotation by π along the z axis. Consequently, if continuous, this transition should belong to the Ising universality class in dimension $d + 1$. The scaling analysis shown in Fig. 4 indicates that this transition is most likely continuous away from the FP and AFM-z phases. However, our magnetization vs field curves indicate that it becomes weakly first order near the boundaries with these two phases, implying that the upper end of the FNM to AFM-xy phase boundary is a CEP, while the lower end corresponds to a triple point (TP) at the junction of the FNM, AFM-xy, and AFM-z phases (see Fig. 1).

The continuous or quasicontinuous nature of the FNM to AFM-xy quantum phase transition indicates that the single-boson condensate is continuously converted into a condensate of pairs (the condensate density is equal to the particle density $\rho = 1 - m_z$ in the low-density limit). This observation implies that BECs of pairs and single bosons coexist in a finite region of the AFM-xy phase that ends up at the phase boundary between the two phases where the single-boson BEC disappears completely: $\langle S_j^+ \rangle = 0$. Indeed, for $d = 3$ and $D = -6.3J$, the size of the boson-pair $\xi \simeq 0.77$ is three times shorter than the average interboson distance $\rho^{-1/3}$ right below the saturation field ($\rho = 1 - m_z \simeq 0.1$).

The AFM-xy and FNM orderings correspond to BECs of single bosons and pairs of bosons, respectively. The shape of the phase boundary opens the possibility of measuring magnetic field induced transitions between these two phases [see Figs. 1(a) and 1(b)]. Since a direct experimental detection of the spin-nematic order parameter can be rather challenging, our predictions for the quantum phase diagram and behavior of different thermodynamic properties are crucial for unveiling this ordering in real magnets. While many $S = 1$ magnets are described by $\mathcal{H}$,[26–29] it is vital to know what are the optimal ratios of D/J for detecting the FNM ordering and characterizing the FNM to AFM-xy quantum phase transition. Since most of these compounds are organic magnets, the D/J ratio can be largely tuned as a function of pressure. Thus, knowing the appropriate range of D/J values is necessary for detecting organic materials in which such a transition can be induced by pressure in magnetic fields that should be nearly 95% of the saturation field.

Finally, we mention that field-induced spin supersolid states (coexistence of AFM-z and FNM orderings) exist at least in the strongly anisotropic limit of $\mathcal{H}$ for triangular[30–32] and face-centered-cubic lattices.[33] Other exotic states have been reported for the kagome lattice.[20] Ferronematic order has also been obtained for $S = 1$ Heisenberg models that include biquadratic interactions.[10,34–37]

We thank A. Paduan-Filho and J. Manson for valuable comments. This research used resources of the National Energy Research Scientific Computing Center (NERSC), which is supported by the Office of Science of the U.S. Department of Energy under Contract No. DE-AC02-05CH11231. Work at LANL was performed under the auspices of a J. Robert Oppenheimer Fellowship and the U.S. DOE Contract No. DE-AC52-06NA25396 through the LDRD program.

[1] M. H. Anderson, J. R. Ensher, M. R. Matthews, C. E. Wieman, and E. A. Cornell, Science **269**, 198 (1995).

[2] K. B. Davis, M. O. Mewes, M. R. Andrews, N. J. van Druten, D. S. Durfee, D. M. Kurn, and W. Ketterle, Phys. Rev. Lett. **75**, 3969 (1995).

[3] T. Nikuni, M. Oshikawa, A. Oosawa, and H. Tanaka, Phys. Rev. Lett. **84**, 5868 (2000).

[4] M. Jaime, V. F. Correa, N. Harrison, C. D. Batista, N. Kawashima, Y. Kazuma, G. A. Jorge, R. Stern, I. Heinmaa, S. A. Zvyagin *et al.*, Phys. Rev. Lett. **93**, 087203 (2004).

[5] V. S. Zapf, D. Zocco, B. R. Hansen, M. Jaime, N. Harrison, C. D. Batista, M. Kenzelmann, C. Niedermayer, A. Lacerda, and A. Paduan-Filho, Phys. Rev. Lett. **96**, 077204 (2006).

[6]S. Sebastian, N. Harrison, C. Batista, L. Balicas, M. Jaime, P. Sharma, N. Kawashima, and I. Fisher, Nature (London) **441**, 617 (2006).
[7]T. Giamarchi, C. Rüegg, and O. Tchernyshyov, Nat. Phys. **4**, 198 (2008).
[8]S. E. Sebastian, P. Tanedo, P. A. Goddard, S.-C. Lee, A. Wilson, S. Kim, S. Cox, R. D. McDonald, S. Hill, N. Harrison *et al.*, Phys. Rev. B **74**, 180401 (2006).
[9]T. Matsubara and H. Matsuda, Prog. Theor. Phys. **16**, 569 (1956).
[10]C. D. Batista and G. Ortiz, Adv. Phys. **53**, 1 (2004).
[11]S. Diehl, M. Baranov, A. J. Daley, and P. Zoller, Phys. Rev. Lett. **104**, 165301 (2010).
[12]Y.-W. Lee and M.-F. Yang, Phys. Rev. A **81**, 061604 (2010).
[13]L. Bonnes and S. Wessel, Phys. Rev. Lett. **106**, 185302 (2011).
[14]K.-K. Ng and M.-F. Yang, Phys. Rev. B **83**, 100511 (2011).
[15]Y.-C. Chen, K.-K. Ng, and M.-F. Yang, Phys. Rev. B **84**, 092503 (2011).
[16]P. Sengupta and C. D. Batista, Phys. Rev. Lett. **99**, 217205 (2007).
[17]P. Sengupta and C. D. Batista, Phys. Rev. Lett. **98**, 227201 (2007).
[18]D. Peters, I. P. McCulloch, and W. Selke, Phys. Rev. B **79**, 132406 (2009).
[19]C. J. Hamer, O. Rojas, and J. Oitmaa, Phys. Rev. B **81**, 214424 (2010).
[20]K. Damle and T. Senthil, Phys. Rev. Lett. **97**, 067202 (2006).
[21]N. Kawashima and K. Harada, J. Phys. Soc. Jpn. **73**, 1379 (2004).
[22]Y. Kato, arXiv:1211.1627.
[23]O. F. Syljuåsen and A. W. Sandvik, Phys. Rev. E **66**, 046701 (2002).
[24]E. L. Pollock and D. M. Ceperley, Phys. Rev. B **36**, 8343 (1987).
[25]A. Pelissetto and E. Vicari, Phys. Rep. **368**, 549 (2002).
[26]C. C. Becerra, N. F. Oliveira, A. Paduan-Filho, W. Figueiredo, and M. V. P. Souza, Phys. Rev. B **38**, 6887 (1988).
[27]A. Wiedenmann, L. Regnault, P. Burlet, J. Rossat-Mignod, O. Kound, and D. Billerey, Physica B: Condens. Matter **156–157**, 305 (1989).
[28]K. Katsumata, M. Hagiwara, M. Tokunaga, and H. Yamaguchi, J. Appl. Phys. **87**, 5085 (2000).
[29]C. O'Connor, S. Bhatia, R. L. Carlin, A. van der Bilt, and A. van Duyneveldt, Physica B + C **95**, 23 (1978).
[30]M. Boninsegni and N. Prokof'ev, Phys. Rev. Lett. **95**, 237204 (2005).
[31]S. Wessel and M. Troyer, Phys. Rev. Lett. **95**, 127205 (2005).
[32]D. Heidarian and K. Damle, Phys. Rev. Lett. **95**, 127206 (2005).
[33]T. Suzuki and N. Kawashima, Phys. Rev. B **75**, 180502 (2007).
[34]K. Harada and N. Kawashima, Phys. Rev. B **65**, 052403 (2002).
[35]T. A. Tóth, A. M. Läuchli, F. Mila, and K. Penc, Phys. Rev. B **85**, 140403(R) (2012).
[36]A. Läuchli, G. Schmid, and S. Trebst, Phys. Rev. B **74**, 144426 (2006).
[37]S. R. Manmana, A. M. Läuchli, F. H. L. Essler, and F. Mila, Phys. Rev. B **83**, 184433 (2011).